

Altered Calcium Channel Currents in Purkinje Cells of the Neurological Mutant Mouse *leaner*

Nancy M. Lorenzon,¹ Cathleen M. Lutz,² Wayne N. Frankel,² and Kurt G. Beam¹

¹Department of Anatomy and Neurobiology, Colorado State University, Fort Collins, Colorado 80523, and ²The Jackson Laboratory, Bar Harbor, Maine 04609

Mutations of the α_{1A} calcium channel subunit have been shown to cause such human neurological diseases as familial hemiplegic migraine, episodic ataxia-2, and spinocerebellar ataxia 6 and also to cause the murine neurological phenotypes of *tottering* and *leaner*. The *leaner* phenotype is recessive and characterized by ataxia with cortical spike and wave discharges (similar to absence epilepsy in humans) and a gradual degeneration of cerebellar Purkinje and granule cells. The mutation responsible is a single-base substitution that produces truncation of the normal open reading frame beyond repeat IV and expression of a novel C-terminal sequence. Here, we have used whole-cell recordings to determine whether the *leaner* mutation alters calcium channel currents in cerebellar Purkinje cells, both because these cells are profoundly affected in *leaner* mice and

because they normally express high levels of α_{1A} . In Purkinje cells from normal mice, 82% of the whole-cell current was blocked by 100 nM ω -agatoxin-IVA. In Purkinje cells from homozygous *leaner* mice, this ω -agatoxin-IVA-sensitive current was 65% smaller than in control cells. Although attenuated, the ω -agatoxin-IVA-sensitive current in homozygous *leaner* cells had properties indistinguishable from that of normal Purkinje neurons. Additionally, the ω -agatoxin-IVA-insensitive current was unaffected in homozygous *leaner* mice. Thus, the *leaner* mutation selectively reduces P-type currents in Purkinje cells, and the α_{1A} subunit and P-type current appear to be essential for normal cerebellar function.

Key words: calcium channel; cerebellum; Purkinje cell; neurological disorders; mutant mice; ω -agatoxin-IVA

Recently, mutations in the α_{1A} calcium channel subunit have been shown to produce the human neurological disorders of autosomal dominant spinocerebellar ataxia (Zhuchenko et al., 1997), familial hemiplegic migraine, and episodic ataxia type-2 (Ophoff et al., 1996). In each of these diseases, alterations of a single gene result in a host of aberrant neurological phenotypes including abnormal cerebellar function and cerebellar atrophy. Defects in the gene encoding the α_{1A} calcium channel subunit are also responsible for the phenotypes of *tottering* (*tg*) and *leaner* (*tg^{la}*) mutant mice. The *tg^{la}* mutation has been identified as a single-base pair substitution in a splice donor consensus sequence of the gene for the α_{1A} subunit, which results in a truncation in the normal open reading frame beyond repeat IV and expression of a novel C-terminal sequence (Fletcher et al., 1996; Doyle et al., 1997).

The *tg^{la}* mutation is inherited as a recessive trait, and homozygous mutants are severely ataxic with cortical spike and wave discharges similar to absence epilepsy in humans (Noebels, 1984). The *tg^{la}* mutation is also associated with cerebellar atrophy resulting from a gradual degeneration of cerebellar Purkinje and granule cells. The cerebella of *tg^{la}/tg^{la}* mice contain 80% fewer Purkinje cells compared with those of normal mice (Herrup and Wilczynski, 1982), and the surviving Purkinje cells exhibit aberrant morphology of the dendritic tree and axonal swellings (Heckroth and Abbott, 1994).

Normally, α_{1A} channels are highly expressed in cerebellar Purkinje cells (Mori et al., 1991; Starr et al., 1991; Stea et al.,

1994; Westenbroek et al., 1995). This, together with the observation that low concentrations of ω -agatoxin-IVA block ~90% of the calcium channel current in Purkinje cells (Mintz et al., 1992b), has been the basis for the assumption that α_{1A} encodes P-type channels (which are defined by block with low concentrations of ω -agatoxin-IVA). However, heterologous expression of the α_{1A} subunit produces a current that (1) is not blocked by low ω -agatoxin-IVA and (2) physiologically resembles the Q-type current recorded from cerebellar granule cells (Sather et al., 1993; Stea et al., 1994). These findings have led to the suggestion that α_{1A} encodes Q-type channels (in addition to its presumed encoding of P-channels). Here we have used whole-cell recordings to determine whether the *tg^{la}* mutation nonspecifically alters calcium channel currents in cerebellar Purkinje cells or affects only P-type current as defined by sensitivity to ω -agatoxin-IVA.

We report here that the *tg^{la}* mutation causes a marked reduction of P-type current in cerebellar Purkinje cells, and that non-P-type currents are unaffected by the *tg^{la}* mutation. Thus, α_{1A} most likely does encode P-type channels. It remains to be determined why a decrease in P-type calcium current ultimately causes the disease phenotype.

MATERIALS AND METHODS

Mutant mice. C57BL/6J mice (breeding pairs of *tg^{la}/+*, *+/Os*, and *+/+* mice) were provided from colonies at The Jackson Laboratory (Bar Harbor, ME). *Os* is a tightly linked, semidominant skeletal mutation carried in repulsion with *tg^{la}*. Heterozygous *Os/+* mice, identified by the oligosyndactylism, were inferred to be heterozygous for the *tg^{la}* mutation. Mice with no oligosyndactylism were inferred to be homozygous for the *tg^{la}* mutation. Because homozygous *Os/Os* is embryonic lethal, we used pups from C57BL/6J wild-type matings as normal controls (without the *tg^{la}* or *Os* mutation). Cells were isolated from 1-week-old mice (P7–P9). This age precedes Purkinje cell death [marked Purkinje cell loss is observed at approximately postnatal day 40 (P40); granule cell death

Received Jan. 27, 1998; revised March 30, 1998; accepted April 1, 1998.

This work was supported by National Institutes of Health Grant NS24444 to K.G.B. We gratefully acknowledge the excellent technical assistance of K. Lopez-Jones and K. Parsons. We are grateful to Pfizer, Inc. for a gift of ω -agatoxin-IVA.

Correspondence should be addressed to Kurt G. Beam, Department of Anatomy and Neurobiology, Colorado State University, Fort Collins, CO 80523.

Copyright © 1998 Society for Neuroscience 0270-6474/98/184482-08\$05.00/0

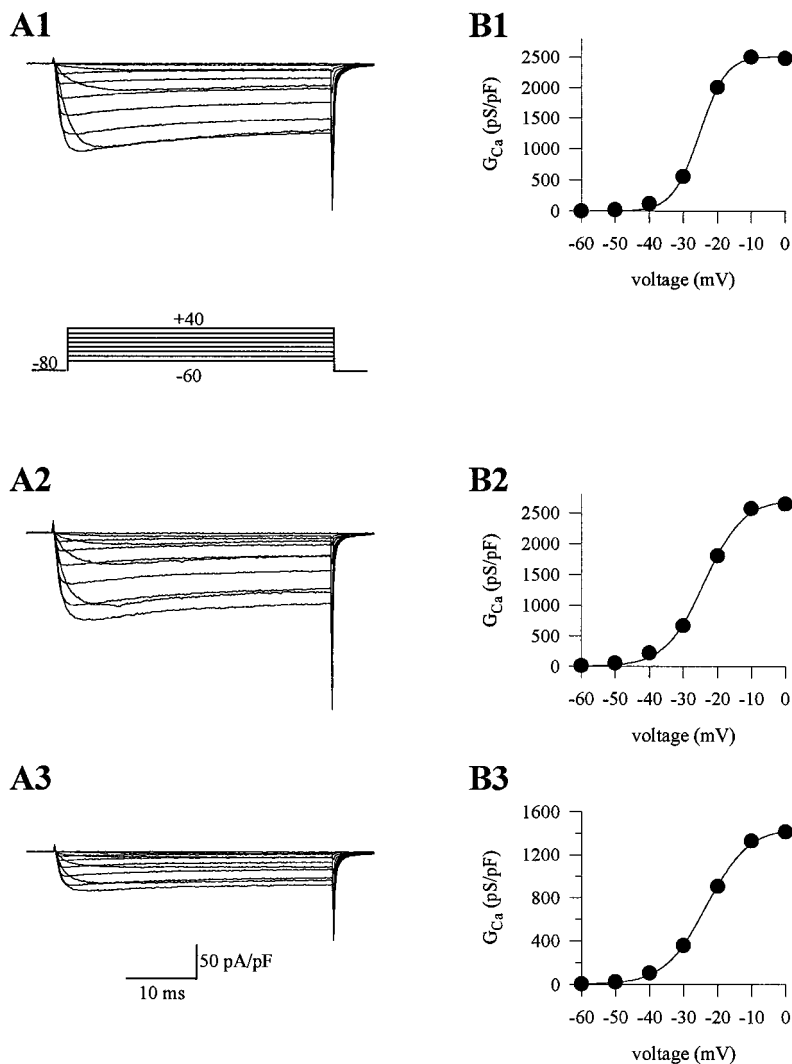


Figure 1. Barium currents in Purkinje cells of wild-type and *leaner* mice. *A1–A3*, Inward currents elicited by depolarizing voltage steps from a holding potential of -80 mV in wild-type (*A1*), $tg^{la/+}$ (*A2*), and $tg^{la/tg^{la}}$ (*A3*) cells. Note the difference in current densities between cell types (I_{pk} for wild-type = -134.3 pA/pF, $tg^{la/+}$ = -132.7 pA/pF, and $tg^{la/tg^{la}}$ = -70.4 pA/pF). *B1–B3*, Conductance versus voltage curves plotted from currents in *A1–A3*. The data were fitted with a single Boltzmann function. The G - V curves had similar half-activation voltages (for wild-type cell, $V_{1/2}$ = -25.3 mV; $tg^{la/+}$ cell, $V_{1/2}$ = -23.9 mV; $tg^{la/tg^{la}}$ cell, $V_{1/2}$ = -23.2 mV). The slope factor of the $tg^{la/tg^{la}}$ curve (6.2) was greater than that for the $tg^{la/+}$ (5.7) and wild-type cells (3.9).

begins at approximately P10 (Herrup and Wilczynski, 1982)] but is a stage when acutely dissociated Purkinje cells can be easily identified morphologically.

Dissociation of neurons. Mouse cerebellar Purkinje cells were acutely isolated using a procedure modified from Mintz et al. (1992b). Briefly, cerebella were removed from P7–P9 mice in an ice-cold solution containing (in mM): 82 Na_2SO_4 , 30 K_2SO_4 , 5 $MgCl_2$, 10 HEPES, and 10 glucose, pH 7.4. The tissue was cut into small pieces and then placed into the same high-Na/high-K solution with enzyme (protease type XXIII; Sigma, St. Louis, MO; 3.0 mg/ml at 37°C). After 7–8 min, the tissue was washed two times in the high-Na/high-K solution without enzyme. The tissue was triturated with a fire-polished Pasteur pipette in minimum essential medium (Life Technologies, Grand Island, NY) containing 1 mg/ml trypsin inhibitor type II-0 (Sigma), 1 mg/ml bovine serum albumin (Sigma), 15 mM HEPES, and 10 mM glucose, pH 7.4. The cell suspension was transferred to poly-L-lysine-coated plastic Petri dishes and remained in the trituration solution at room temperature until just before electrophysiological recording. Purkinje cells were identified by the morphological characteristics of relatively large size and apical dendritic stump (Regan, 1991; Mintz et al., 1992b).

Recording solutions and pharmacological agents. Calcium channel currents were isolated using an external solution that included (in mM): 160 TEA-Cl, 5 $BaCl_2$, and 10 HEPES, pH 7.4, and an internal solution that consisted of (in mM): 108 Cs-methanesulfonate, 4 $MgCl_2$, 9 HEPES, 9 EGTA, 14 phosphocreatine, 0.3 GTP, and 4 ATP, pH 7.4. ω -Agatoxin-IVA (ω -AgTx-IVA; a gift from Pfizer, Groton, CT; or purchased from Peptides International, Louisville, KY) was prepared as a concentrated stock in distilled water with 1 mg/ml bovine serum albumin and then stored as aliquots at $-80^\circ C$. The calcium channel antagonist was diluted

in the external recording solution on the day of the experiment. Drugs were delivered with a multibarrel array (“sewer pipe”) of glass capillary tubing (150 μm outer diameter) mounted on a micromanipulator.

Whole-cell patch-clamp recordings. Whole-cell recordings were obtained using conventional techniques (Hamill et al., 1981) at room temperature with a Dagan 3900 patch-clamp amplifier and a 3911 whole-cell expander. Electrodes (1–3 M) were pulled from soda lime glass with a Brown-Flaming puller (Sutter) and coated with wax to reduce capacitance. After attainment of a gigaohm seal and entry into whole-cell mode, series resistance was compensated electronically. Linear leak and capacitive currents were removed by digital subtraction of scaled control currents (evoked by a 20 mV hyperpolarizing voltage step from the holding potential). Data acquisition and analysis were performed with software programs written in BASIC-23. Current densities were calculated by dividing the current amplitude by the linear capacitance of the cell. All summary data are presented as mean \pm SEM (number of cells), and population data were compared with the use of an unpaired Student’s t test.

RESULTS

Barium currents were recorded from cerebellar Purkinje cells of homozygous *leaner* ($tg^{la/tg^{la}}$), heterozygous *leaner* ($tg^{la/+}$), and wild-type mice. Barium currents from $tg^{la/tg^{la}}$ mice appeared qualitatively similar to those from $tg^{la/+}$ and wild-type mice. Thus, in neurons of all three genotypes, a sustained inward current was activated by depolarizing voltage steps from a holding potential of -80 mV (Fig. 1). With 5 mM Ba^{2+} as the charge

Table 1. Biophysical properties of total barium currents in wild-type and *leaner* Purkinje cells

	Wild-type	<i>tg^{la}/+</i>	<i>tg^{la}/tg^{la}</i>
Total I_{Ba} density (pA/pF)	186.2 ± 10.0 (22)	140.3 ± 5.2 (35)*	61.5 ± 2.6 (51)*
Voltage dependence of activation			
$V_{1/2}$ (mV)	−22.5 ± 1.6 (8)	−21.9 ± 1.2 (14)	−24.8 ± 1.0 (18)
Slope factor (mV)	4.0 ± 0.2 (8)	4.9 ± 0.3 (14)	6.9 ± 0.2 (18)*
Percent inactivation (%) ^a	63 ± 2 (14)	60 ± 2 (23)	50 ± 2 (31)**
Voltage dependence of inactivation			
$V_{1/2}$ (mV)	−53.0 ± 2.9 (9)	−50.5 ± 2.1 (17)	−56.2 ± 2.7 (20)
Slope factor (mV)	21.1 ± 1.8 (9)	17.9 ± 0.6 (17)	17.8 ± 0.7 (20)
Percent current reduction by 100 nM ω -AgTx IVA (%)	82.1 ± 2.3 (3)	79.7 ± 1.2 (10)	49.1 ± 12.5 (7)*

Values are means ± SEM with number of cells in parentheses.

^aPercent inactivation defined as $[(I_{peak} - I \text{ at } 2 \text{ sec})/I_{peak}]$.

*Significantly different from other groups; $p < 0.0001$.

**Significantly different from other groups; $p < 0.0005$.

carrier, the whole-cell current first activated at approximately −45 mV and reached maximum amplitude at approximately −10 mV. The half-activation voltages of barium currents were also similar in *tg^{la}/tg^{la}*, *tg^{la}/+*, and wild-type cells. A small reduction in the slope of the conductance–voltage (G – V) curve was observed in *tg^{la}/tg^{la}* cells compared with *tg^{la}/+* and wild-type cells (Table 1). However, the most striking alteration in the calcium channel currents of *tg^{la}/tg^{la}* cells was a marked reduction in the peak current density as compared with *tg^{la}/+* and wild-type cells (Table 1). Specifically, the current density in *tg^{la}/tg^{la}* cells was only about half that in *tg^{la}/+* and wild-type cells (51 and 44%, respectively).

To examine the voltage dependence of inactivation, a two-pulse protocol was applied; 2 sec depolarizing prepulses to various potentials (−110 to +30 mV) were followed by a voltage step to the test potential eliciting maximal current in that cell (with a 10 sec interval between inactivation measurements; Fig. 2). The peak current amplitude during the test pulse was measured, and inactivation curves were constructed. The voltage dependence of inactivation did not differ significantly between *tg^{la}/tg^{la}* and control currents (Table 1). However, the ratio of the peak current amplitude to the current amplitude at the end of a 2 sec pulse was greater in *tg^{la}/tg^{la}* Purkinje cells (Fig. 2, Table 1). This could indicate a difference in kinetic properties of the mutant channels. Alternately, it could indicate that the *tg^{la}* mutation decreased the fractional contribution of α_{1A} channels to the total current, so that the whole-cell current became dominated by current through non- α_{1A} channels with a greater ratio of peak to 2 sec current amplitude.

The *tg^{la}* mutation strongly attenuates the P-type current in Purkinje cells

To determine the specific effects of the α_{1A} mutation on P-type currents, barium currents in *tg^{la}/tg^{la}* and control Purkinje cells were recorded before and after the application of ω -AgTx-IVA, and the difference currents were analyzed. ω -AgTx-IVA was applied to the cells at a concentration of 100 nM to ensure that all P-type channels were blocked, because previous studies have shown that 50 nM ω -AgTx-IVA produces maximal block of all non-L-type and non-N-type currents in rat cerebellar Purkinje cells, with no further inhibition by 200 nM toxin (Mintz et al., 1992b). The percentage of the current blocked by 100 nM ω -AgTx-IVA was significantly greater in wild-type and *tg^{la}/+* cells compared with *tg^{la}/tg^{la}* cells (Table 1). The current remain-

ing after application of ω -AgTx-IVA had similar kinetics and density in *tg^{la}/tg^{la}* and control cells, suggesting that the reduction of the α_{1A} current does not affect the remaining, non-P/Q current types in Purkinje cells (Figs. 3A, 4). Thus, the ω -AgTx-IVA-sensitive current (determined by subtraction of the currents recorded after application of ω -AgTx-IVA from control records obtained before ω -AgTx-IVA) is selectively reduced by the *tg^{la}* mutation (Figs. 3B, 4). Despite the difference in amplitude, the ω -AgTx-IVA-sensitive current exhibited a similar time course in *tg^{la}/tg^{la}* and control cells (Fig. 3B). When the ω -AgTx-IVA-sensitive currents in the *tg^{la}/+* and *tg^{la}/tg^{la}* cells were scaled by current amplitude, the traces closely superimposed (Fig. 3D).

To determine the effects of the *tg^{la}* mutation more directly, we characterized the barium current flowing through the α_{1A} channels in isolation (ω -AgTx-IVA-sensitive currents). The ω -AgTx-IVA-sensitive currents in *tg^{la}/+* and *tg^{la}/tg^{la}* cells exhibited no differences in the voltage dependence of activation (Fig. 5). The half-activation voltage of the ω -AgTx-IVA-sensitive current was -22.7 ± 1.9 mV ($n = 7$) in *tg^{la}/+* cells and -22.5 ± 1.9 mV ($n = 6$) in *tg^{la}/tg^{la}* cells. The slopes of the G – V curve for *tg^{la}/+* and *tg^{la}/tg^{la}* currents were 4.3 ± 0.2 ($n = 7$) and 4.5 ± 0.1 ($n = 6$), respectively. Thus, the decreased slope of the G – V curve for the whole-cell currents in *tg^{la}/tg^{la}* cells was not a reflection of altered biophysical properties of the α_{1A} channels associated with the *tg^{la}* mutation.

The inactivation characteristics of the ω -AgTx-IVA-sensitive currents also appeared similar in *tg^{la}/tg^{la}* and control cells, as indicated both by the voltage dependence of inactivation (Fig. 6) and by the ratio of peak current amplitude to current amplitude at 2 sec (0.56 ± 0.04 ; $n = 4$ for *tg^{la}/+* cells; vs 0.51 ± 0.06 ; $n = 4$ for *tg^{la}/tg^{la}* cells). Therefore, the only alteration in the calcium channel current directly caused by the mutation appeared to be the substantial reduction in P-type current density. The small differences in the whole-cell calcium channel current of *tg^{la}/tg^{la}* cells (reduced G – V slope and altered current time course during a 2 sec pulse) evidently resulted from the greater relative proportion of non-P-type calcium channel currents in these cells.

DISCUSSION

Calcium channel currents in *tg^{la}/tg^{la}* mice

We have compared calcium channel currents in Purkinje cells from wild-type mice and mice homozygous for the *tg^{la}* mutation

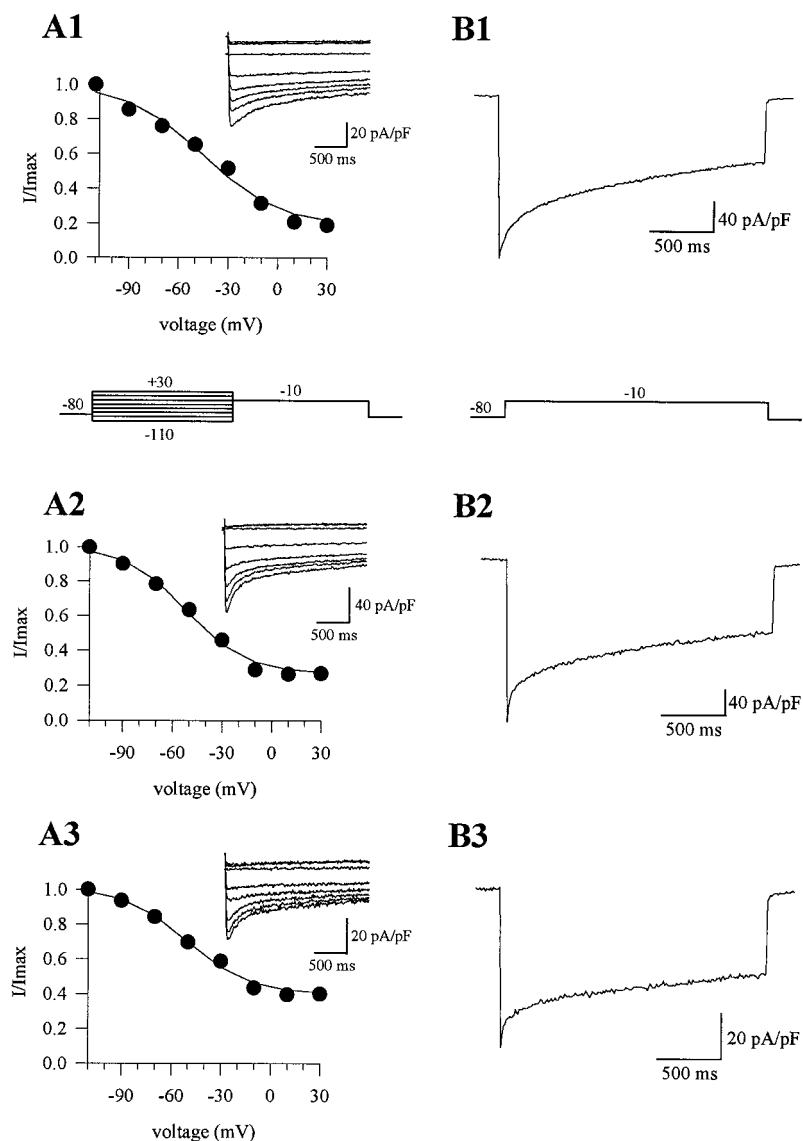


Figure 2. Inactivation of barium currents in wild-type and *leaner* cells. *A1–A3*, Currents elicited by a two-pulse protocol: 2 sec depolarizing prepulses (–110 to 30 mV) followed by a test pulse to –10 mV with a 10 sec time interval between measurements. Peak current density during the test pulse was used to plot inactivation curves (I/I_{max} vs prepulse voltage; data were fit with a single Boltzmann function). The half-inactivation voltages of the inactivation curves were –46.2 mV (slope factor, 18.8) for the wild-type cell (*A1*), –52.3 mV (slope factor, 18.4) for the $tg^{la}/+$ cell (*A2*), and –50.7 mV (slope factor, 19.1) for the tg^{la}/tg^{la} cell (*A3*). *B1–B3*, Barium currents elicited by a long 2 sec depolarizing voltage step to –10 mV. Percent inactivation was 69% in the wild-type cell (*B1*), 55% in the $tg^{la}/+$ cell (*B2*), and 46% in the tg^{la}/tg^{la} cell (*B3*). The same cells were used in *A* and *B*.

of the α_{1A} gene. This tg^{la} mutation specifically reduces the amplitude of P-type current without changing its macroscopic properties. Non-P-type currents are unaffected by the mutation.

Although our electrophysiological measurements cannot determine the specific cause of the attenuated P-type current, we hypothesize that the tg^{la} mutation causes reduced expression of α_{1A} . This hypothesis is supported by the observation that cerebella of tg^{la}/tg^{la} mice express reduced levels of α_{1A} mRNA at all ages tested (embryonic day 10.5 to adult; Doyle et al., 1997). Western blot analysis would reveal whether this reduction in α_{1A} transcript results in reduced α_{1A} protein. In addition to an altered level of channel expression, it might also be that the tg^{la} mutation results in altered subcellular distribution, a possibility which could be examined with immunohistochemistry.

Relationship of P/Q current to the α_{1A} subunit

P- and Q-type calcium currents are differentiated mainly on the basis of pharmacology. Calcium channel current through P-type channels is not sensitive to dihydropyridines or ω -conotoxin-GVIA but is blocked by funnel web spider venom or low concentrations of a component of the venom, ω -AgTx-IVA (Llinas et al., 1989; Mintz et al., 1992a). Q-type current is defined on the

basis of block by high concentrations of ω -AgTx-IVA or ω -conotoxin-MVIIC (Hillyard et al., 1992; Sather et al., 1993; Randall and Tsien, 1995). However, the molecular identity of the channels that carry P- and Q-type currents has been questioned. The α_{1A} subunit was originally thought to encode a P-type channel (Mori et al., 1991), but when expressed in *Xenopus*, the α_{1A} channel has different characteristics (Sather et al., 1993; Stea et al., 1994) resembling the Q-type current recorded in cerebellar granule cells (Randall and Tsien, 1995). It is currently unclear whether the P- and Q-type currents actually arise from different α_1 genes, alternatively spliced forms of the same gene, or the same α_{1A} subunit that is modulated differently by auxiliary subunits. In a recent study using antisense oligonucleotides, Gillard et al. (1997) suggested that P-type current in cerebellar Purkinje cells is encoded by the α_{1A} subunit. Our experiments on the tg^{la}/tg^{la} mouse support the argument that α_{1A} channels are responsible for P-type current in these cells. To determine whether α_{1A} channels also carry Q-type current, future investigation of the calcium channel currents in cerebellar granule cells from tg^{la}/tg^{la} mice would be valuable, because Q-type current is a high percentage of the total calcium channel current in this cell type.

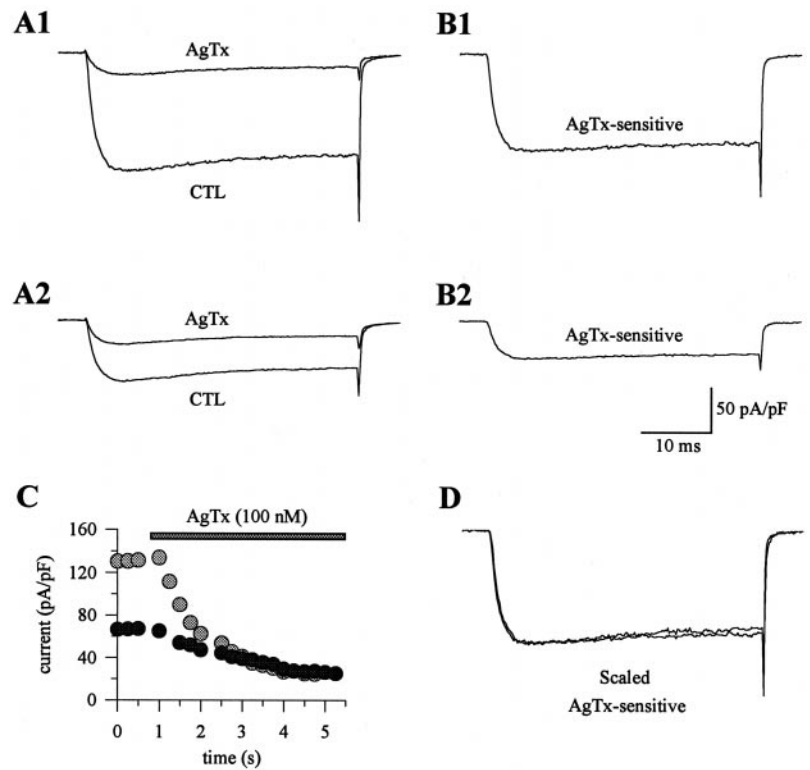


Figure 3. Effects of ω -AgTx-IVA on barium currents in wild-type and *leaner* Purkinje cells. *A1, A2*, Barium currents before and after application of 100 nM ω -AgTx-IVA. ω -AgTx-IVA blocked 82% of the current in the $tg^{la}/+$ cell (*A1*) and 63% in the tg^{la}/tg^{la} cell (*A2*). Note the similarities of the currents resistant to ω -AgTx-IVA in *A1* and *A2*. The current densities of the ω -AgTx-IVA-resistant current were -24.2 pA/pF for the $tg^{la}/+$ cell and -25.2 pA/pF for the tg^{la}/tg^{la} cell. The current remaining after ω -AgTx-IVA block represents non-P-type currents. *B1, B2*, ω -AgTx-IVA-sensitive currents were derived by subtracting the control and ω -AgTx-IVA traces in *A1* and *A2*. The ω -AgTx-IVA-sensitive current from the $tg^{la}/+$ cell had a density of -107.1 pA/pF (*B1*), and that from the tg^{la}/tg^{la} cell was -37.5 pA/pF (*B2*). *C*, Plot of the peak current density versus time for the cells in *A1* and *A2*. Gray circles represent data from the $tg^{la}/+$ cell in *A1*, and the black circles were from the tg^{la}/tg^{la} cell in *A2*. *D*, ω -AgTx-IVA-sensitive currents from *B1* and *B2* were scaled and superimposed.

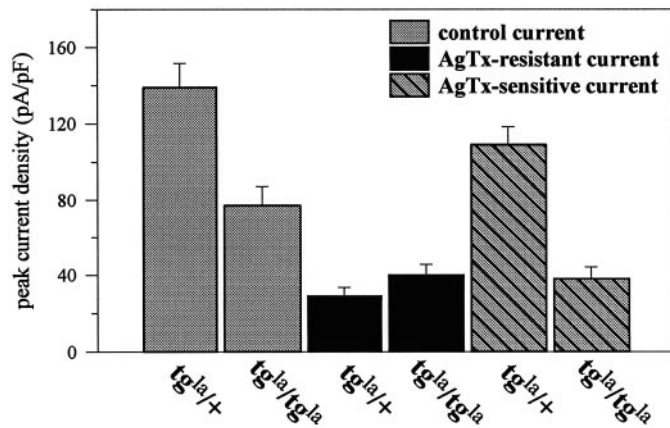


Figure 4. The bar graph depicts the current density of the barium currents in wild-type and *leaner* Purkinje cells. The total barium current densities in tg^{la}/tg^{la} cells were reduced compared with $tg^{la}/+$ cells (gray bars; $p < 0.01$). There was no significant difference between the current densities of the ω -AgTx-IVA-resistant currents (the current remaining after ω -AgTx-IVA block; black bars) in $tg^{la}/+$ and tg^{la}/tg^{la} cells. The mean current density of the ω -AgTx-IVA-sensitive current (striped bars) in tg^{la}/tg^{la} cells was 65% smaller than that in $tg^{la}/+$ cells ($p < 0.0001$).

Effects of the tg^{la} mutation on cellular function

With regard to the pathological consequences of the channel mutation, the question arises: why does a decrease in calcium current density ultimately result in cell death? Several studies have suggested that not only high intracellular calcium concentrations, but also low intracellular calcium levels can result in cell death (Koike et al., 1989; McCaslin and Smith, 1990; Koh and Cotman, 1992). This explanation is insufficient, however, to explain why the Purkinje cell loss in the tg^{la}/tg^{la} mouse is restricted to alternating sagittal compartments of the cerebellar cortex. The

subpopulation of Purkinje cells that survive in tg^{la}/tg^{la} mice appears to be the same population of neurons expressing Zeb1 and displaying abnormal persistent expression of tyrosine hydroxylase (normally Purkinje cells only express tyrosine hydroxylase from the third to fifth postnatal weeks; Heckroth and Abbott, 1994). What allows these cells to be spared is currently not known. The Purkinje cells that are spared in the tg^{la}/tg^{la} cerebellum have abnormal morphology of their dendritic trees and axonal swellings. Because voltage-gated calcium channels are important for growth cone function in neurons (Williams et al., 1992), it is likely that α_{1A} channels are important for dendritic growth and development in Purkinje cells, thus possibly explaining the abnormal morphological characteristics of Purkinje cells in tg^{la}/tg^{la} mice.

Immunolocalization in normal mice reveals pronounced α_{1A} staining in terminals along dendrites of cerebellar Purkinje cells, hippocampal neurons, and cortical pyramidal neurons (Westenbroek et al., 1995). The pharmacological block of P/Q currents inhibits transmission at various synapses in the central and peripheral nervous systems (Luebke et al., 1993; Regehr and Mintz 1994; Wheeler et al., 1994; Bowersox et al., 1995). Thus, a decrease in calcium current density in tg^{la}/tg^{la} mice would most likely attenuate synaptic transmission at synapses between many cell types.

The attenuation of calcium channel current would also affect other cellular functions, especially in cerebellar Purkinje cells, where α_{1A} channels are additionally distributed along dendrites and in the cell body. α_{1A} channels expressed in Purkinje cell dendrites may play an important role in integration and propagation of synaptic signals (Llinas et al., 1992). However, it is also possible that alterations in calcium current density affect nervous system function via a more indirect route. The aberrant tyrosine hydroxylase expression in tg^{la}/tg^{la} Purkinje cells suggests that the

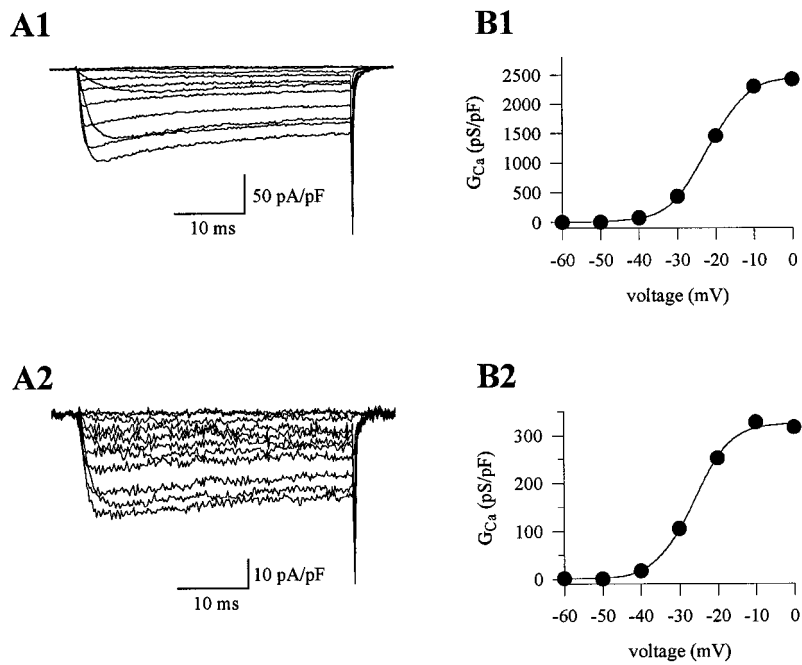


Figure 5. Activation of ω -AgTx-IVA-sensitive currents in $tg^{la}/+$ and tg^{la}/tg^{la} cells. A1, A2, Barium currents elicited by depolarizing voltage steps from a -80 mV holding potential. ω -AgTx-IVA-sensitive currents were derived by subtracting currents recorded after ω -AgTx-IVA block from control currents. Current density was markedly attenuated in the tg^{la}/tg^{la} cell ($I_{pk} = -17.3$ pA/pF) compared with the $tg^{la}/+$ cell ($I_{pk} = -121.3$ pA/pF). B1, B2, G - V curves for the ω -AgTx-IVA-sensitive currents in A1 and A2. Voltage dependence of activation was similar for the $tg^{la}/+$ currents ($V_{1/2} = -21.9$ mV; $k = 5.0$) and the tg^{la}/tg^{la} currents ($V_{1/2} = -26.6$ mV; $k = 4.7$).

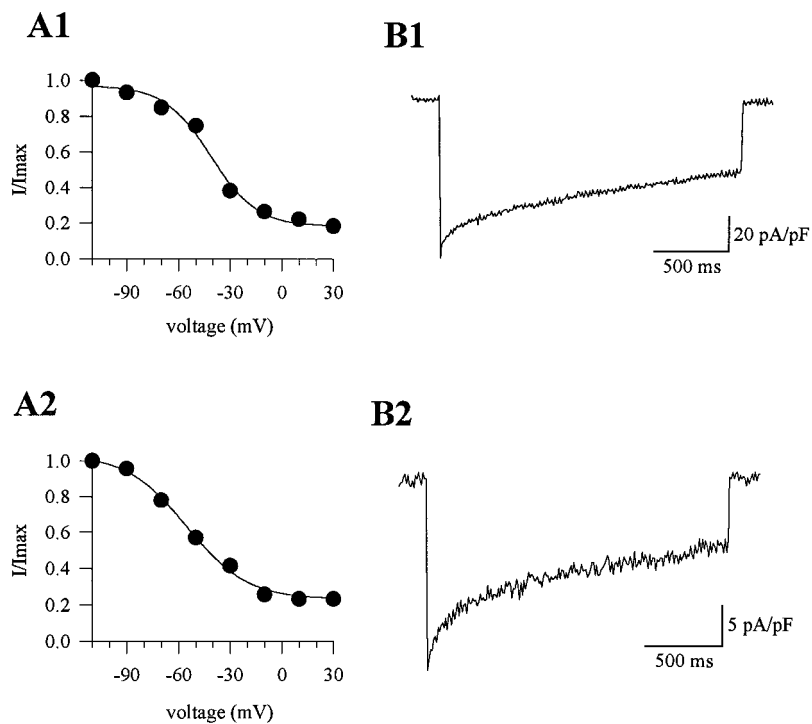


Figure 6. Inactivation properties of ω -AgTx-IVA-sensitive currents in $tg^{la}/+$ and tg^{la}/tg^{la} cells. A1, A2, Voltage dependence of inactivation was described using a Boltzmann function. The $tg^{la}/+$ currents exhibited a half-inactivation voltage of -41.2 mV ($k = 13.2$), and the tg^{la}/tg^{la} currents were half-maximally inactivated at -55.6 mV ($k = 17.4$). B1, B2, Percent inactivation was 51% for the $tg^{la}/+$ current and 67% for the tg^{la}/tg^{la} current.

mutation ultimately causes abnormal developmental signaling such that the mutant cells cannot recognize the signal that down-regulates tyrosine hydroxylase expression (Hess and Wilson, 1991). Although L-type channels have been associated with gene regulation in many neurons (Bading et al., 1993), P-type channels might assume this role in Purkinje cells. This difference can be rationalized on the basis that L-type channels dominate somatically in most CNS neurons, but not in Purkinje cells where the majority of the voltage-gated calcium channels in the soma are P-type.

Other disorders associated with α_{1A} subunit mutations

Tottering (*tg*) is another recessively inherited α_{1A} mutation described in the mouse. The *tg* mutation is a single-nucleotide change resulting in a substitution of leucine for proline in the IIS5-IIS6 linker of the α_{1A} subunit (Fletcher et al., 1996; Doyle et al., 1997). The *tg/tg* mouse resembles the tg^{la}/tg^{la} mouse in having absence seizures. However, these two mutant mice differ in that *tg/tg* mice exhibit only mild ataxia, intermittent focal motor seizures (which are not seen in the tg^{la}/tg^{la} mouse; Noebels, 1984), and minor diffuse loss of cerebellar granule and Purkinje cells. As

in tg^{la}/tg^{la} mice, the Purkinje cells in tg/tg mice aberrantly express tyrosine hydroxylase (Hess and Wilson, 1991).

Several human disorders have been associated with α_{1A} subunit mutations. One of these diseases, autosomal dominant spinocerebellar ataxia (SCA6), is characterized by slowly progressive ataxia, nystagmus, dysarthria, and cerebellar atrophy (with a severe loss of Purkinje cells, moderate loss of granule cells and dentate nucleus neurons, and mild to moderate cell loss in the inferior olive). Genetic analysis of patients with SCA6 disclosed an expansion of a CAG repeat resulting in a polyglutamine expansion (Zhuchenko et al., 1997). Another human neurological disorder associated with an α_{1A} channel mutation is familial hemiplegic migraine (FHM), which presents as ictal hemiparesis, ataxia, nystagmus, and, in some families, cerebellar atrophy. FHM is associated with four different missense mutations in conserved functional domains (Ophoff et al., 1996). A third disorder, episodic ataxia type-2, is associated with cerebellar ataxia, migraine-like symptoms, interictal nystagmus, and cerebellar atrophy and is correlated with two mutations that disrupt the reading frame and cause premature stops so that the channel protein contains only repeats I, II, and part of III (Ophoff et al., 1996).

Another mutant mouse exhibiting some disease traits that overlap with those previously described for α_{1A} human and murine diseases (ataxia and spontaneous focal motor and absence seizures) is the lethargic (*lh*) mouse. However, no pathological changes are observed in the brains of these mutants (Dung and Swigart, 1972). The *lh* mutation is not located in the α_{1A} subunit gene but rather in the gene encoding the β_4 auxiliary subunit that associates with the α_1 subunit. In heterologous expression studies, β subunits have been shown to augment and modulate α_1 calcium channel currents (Hullin et al., 1992; Castellano et al., 1993). The *lh* mutation is a four-nucleotide insertion into a splice donor sequence that results in exon skipping, translational frame shift, and protein truncation with loss of the α_1 -binding site (Burgess et al., 1997). This mutation would cause a functional loss of β_4 , which could ultimately result in altered α_1 calcium channel currents.

In summary, the present study demonstrates that α_{1A} expression and P-type current in cerebellar Purkinje cells are critical for normal cerebellar function. Currently, it is unclear how the tg^{la} mutation of the α_{1A} channel subunit and subsequent decrease in current density cause the mutant phenotypes. This α_{1A} mutation ultimately results in abnormal cellular morphology and function and cell death. Additionally, the mutation most likely causes attenuation of synaptic transmission, alters dendritic integration, and results in abnormal developmental signaling in Purkinje cells. Comparing calcium channel function and the neurological characteristics in different α_{1A} diseases may suggest hypotheses regarding the etiology of these diseases and methods for treatment.

REFERENCES

- Bading H, Ginty DD, Greenberg ME (1993) Regulation of gene expression in hippocampal neurons by distinct calcium signaling pathways. *Science* 260:181–186.
- Bowersox SS, Miljanich GP, Sugiura Y, Li C, Nadasdi L, Hoffman BB, Ramachandran J, Ko C-P (1995) Differential blockade of voltage-sensitive calcium channels at the mouse neuromuscular junction by novel ω -conopeptides and ω -agatoxin-IVA. *J Pharmacol Exp Ther* 273:248–256.
- Burgess DL, Jones JM, Meisler MH, Noebels JL (1997) Mutation of the Ca^{2+} channel β subunit gene *Cchb4* is associated with ataxia and seizures in the lethargic (*lh*) mouse. *Cell* 88:385–392.
- Castellano A, Wei X, Birnbaumer L, Perez-Reyes E (1993) Cloning and expression of a neuronal calcium channel beta subunit. *J Biol Chem* 268:12359–12366.
- Doyle J, Ren X, Lennon G, Stubbs L (1997) Mutations in the *Cacn11a4* calcium channel gene are associated with seizures, cerebellar degeneration, and ataxia in tottering and leaner mutant mice. *Mamm Genome* 8:113–120.
- Dung HC, Swigart RH (1972) Histo-pathologic observations of the nervous and lymphoid tissues of “lethargic” mutant mice. *Tex Rep Biol Med* 30:23–39.
- Fletcher CF, Lutz CM, O’Sullivan TN, Shaughnessy Jr JD, Hawkes R, Frankel WN, Copeland NG, Jenkins N (1996) Absence epilepsy in tottering mutant mice is associated with calcium channel defects. *Cell* 87:607–617.
- Gillard SE, Volsen SG, Smith W, Beattie RE, Bleakman D, Lodge D (1997) Identification of pore-forming subunit of P-type calcium channels: an antisense study on rat cerebellar Purkinje cells in culture. *Neuropharmacology* 36:405–409.
- Hamill OP, Marty A, Neher E, Sakman B, Sigworth FJ (1981) Improved patch-clamp techniques for high-resolution current recording from cells and cell-free membrane patches. *Pflügers Arch* 391:85–100.
- Heckroth JA, Abbott LC (1994) Purkinje cell loss from alternating sagittal zones in the cerebellum of leaner mutant mice. *Brain Res* 658:93–104.
- Herrup K, Wilczynski SL (1982) Cerebellar cell degeneration in the leaner mutant mouse. *Neuroscience* 7:2185–2196.
- Hess EJ, Wilson MC (1991) Tottering and leaner mutations perturb transient developmental expression of tyrosine hydroxylase in embryonically distinct Purkinje cells. *Neuron* 6:123–132.
- Hillyard DR, Monje VD, Mintz IM, Bean BP, Nadasdi L, Ramachandran J, Mijanich G, Azimi-Zoonooz A, McIntosh JM, Cruz LJ, Imperial JS, Olivera BM (1992) A new conus peptide ligand for mammalian presynaptic Ca^{2+} channels. *Neuron* 9:69–77.
- Hullin R, Singer-Lahat D, Freichel M, Biel M, Dascal N, Hofmann F, Flockerzi V (1992) Calcium channel beta subunit heterogeneity: functional expression of cloned cDNA from heart, aorta, and brain. *EMBO J* 11:885–890.
- Koh JY, Cotman CW (1992) Programmed cell death: its possible contribution to neurotoxicity mediated by calcium channel antagonists. *Brain Res* 587:233–240.
- Koike T, Martin DP, Johnson Jr EM (1989) Role of Ca^{2+} channels in the ability of membrane depolarization to prevent neuronal death induced by trophic-factor deprivation: evidence that levels of internal Ca^{2+} determine nerve growth factor dependence of sympathetic ganglion cells. *Proc Natl Acad Sci USA* 86:6421–6425.
- Llinas R, Sugimori M, Lin J-W, Cherksey B (1989) Blocking and isolation of a calcium channel from neurons in mammals and cephalopods utilizing a toxin fraction (FTX) from funnel-web spider poison. *Proc Natl Acad Sci USA* 86:1689–1693.
- Llinas R, Sugimori M, Hillman DE, Cherksey B (1992) Distribution and functional significance of the P-type, voltage-dependent Ca^{2+} channels in the mammalian central nervous system. *Trends Neurosci* 15:351–355.
- Luebke JI, Dunlap K, Turner TJ (1993) Multiple calcium channel types control glutamatergic synaptic transmission in the hippocampus. *Neuron* 11:895–902.
- McCaslin PP, Smith TG (1990) Low calcium-induced release of glutamate results in autotoxicity of cerebellar granule cells. *Brain Res* 53:280–285.
- Mintz IM, Venema VJ, Swiderek KM, Lee TD, Bean BP, Adam ME (1992a) P-type calcium channels blocked by the spider toxin ω -agatoxin-IVA. *Nature* 355:827–829.
- Mintz IM, Adams ME, Bean BP (1992b) P-type calcium channels in rat central and peripheral neurons. *Neuron* 9:85–95.
- Mori Y, Friedrich T, Kim M-S, Mikami A, Nakai J, Ruth P, Bosse E, Hofmann F, Flockzi V, Furuichi T, Mikoshiba K, Imoto K, Tanabe T, Numa S (1991) Primary structure and functional expression from complementary DNA of a brain calcium channel. *Nature* 350:398–402.
- Noebels JL (1984) A single gene error of noradrenergic axon growth synchronizes central neurones. *Nature* 310:4019–411.
- Ophoff RA, Terwindt GM, Vergouwe MN, van Eijk R, Oefner PJ, Hoffman SMG, Lamberdin JE, Mohrenweiser HW, Bulman DE, Ferrari M, Hann J, Lindhout D, van Ommen G-JB, Hofker MH, Ferrari MD, Frants RR (1996) Familial hemiplegic migraine and episodic

- ataxia type-2 are caused by mutations in the Ca^{2+} channel gene CACNL1A4. *Cell* 543–552.
- Randall A, Tsien RW (1995) Pharmacological dissection of multiple types of Ca^{2+} channel currents in rat cerebellar granule neurons. *J Neurosci* 15:2995–3012.
- Regan JJ (1991) Voltage-dependent calcium currents in Purkinje cells from rat cerebellar vermis. *J Neurosci* 11:2259–2269.
- Regehr WG, Mintz IM (1994) Participation of multiple calcium channel types in transmission at single climbing fiber to Purkinje cell synapses. *Neuron* 12:605–613.
- Sather WA, Tanabe T, Zhang J-F, Mori Y, Adams ME, Tsien RW (1993) Distinctive biophysical and pharmacological properties of Class A (B1) calcium channel α_1 subunits. *Neuron* 11:291–303.
- Starr TVB, Prystay W, Snutch TP (1991) Primary structure of a calcium channel that is highly expressed in the rat cerebellum. *Proc Natl Acad Sci USA* 88:5621–5625.
- Stea A, Tomlinson WJ, Soong TW, Bourinet E, Dubel SJ, Vincent SR, Snutch TP (1994) Localization and functional properties of a rat brain α_{1A} calcium channel reflect similarities to neuronal Q- and P-type channels. *Proc Natl Acad Sci USA* 91:10576–10580.
- Westenbroek RE, Sakurai T, Elliott EM, Hell JW, Starr TVB, Snutch TP, Catterall WA (1995) Immunochemical identification and subcellular distribution of the α_{1A} subunits of brain calcium channels. *J Neurosci* 15:6403–6418.
- Wheeler DB, Randall A, Tsien RW (1994) Roles of N-type and Q-type Ca^{2+} channels in supporting hippocampal synaptic transmission. *Science* 264:107–111.
- Williams EM, Doherty P, Turner G, Reid RA, Hemperly JJ, Walsh FS (1992) Calcium influx into neurons can solely account for cell contact-dependent neurite outgrowth stimulated by transfected L1. *Cell Biol* 119:883–892.
- Zhuchenko O, Bailey J, Bonnen P, Ashizawa T, Stockton DW, Amos C, Dobyns WB, Subramony SH, Zoghbi HY, Lee CC (1997) Autosomal dominant cerebellar ataxia (SCA6) associated with small polyglutamine expansions in the α_{1A} -voltage-dependent calcium channel. *Nat Genet* 15:62–69.